The Astrophysical Journal, 816:70 (8pp), 2016 January 10 doi:10.3847/0004-637X/816/2/70

WEIGHING STARS: THE IDENTIFICATION OF AN EVOLVED BLUE STRAGGLER STAR IN THE GLOBULAR CLUSTER 47 TUCANAE*

F. R. Ferraro[1], E. Lapenna[1], A. Mucciarelli[1], B. Lanzoni[1], E. Dalessandro[1], C. Pallanca[1], and D. Massari[2,3]
[1] Dipartimento di Fisica e Astronomia, Università degli Studi di Bologna, Viale Berti Pichat 6/2, I-40127 Bologna, Italy
[2] INAF-Osservatorio Astronomico di Bologna, Via Ranzani 1, I-40127 Bologna, Italy
[3] Kapteyn Astronomical Institute, University of Groningen, P.O. Box 800, 9700 AV Groningen, The Netherlands
Received 2015 October 1; accepted 2015 November 19; published 2016 January 11

ABSTRACT

Globular clusters are known to host peculiar objects named blue straggler stars (BSSs), significantly heavier than the normal stellar population. While these stars can be easily identified during their core hydrogen-burning phase, they are photometrically indistinguishable from their low-mass sisters in advanced stages of the subsequent evolution. A clear-cut identification of these objects would require the direct measurement of the stellar mass. We used the detailed comparison between chemical abundances derived from neutral and from ionized spectral lines as a powerful stellar *"weighing device"* to measure stellar mass and to identify an evolved BSS in 47 Tucanae. In particular, high-resolution spectra of three bright stars, located slightly above the level of the "canonical" horizontal branch (HB) sequence in the color–magnitude diagram of 47 Tucanae, have been obtained with the UVES spectrograph. The measurements of iron and titanium abundances performed separately from neutral and ionized lines reveal that two targets have stellar parameters fully consistent with those expected for low-mass post-HB objects, while for the other target the elemental ionization balance is obtained only by assuming a mass of $\sim 1.4 M_{\odot}$, which is significantly larger than the main sequence turn-off mass of the cluster ($\sim 0.85 M_{\odot}$). The comparison with theoretical stellar tracks suggests that this is a BSS descendant possibly experiencing its core helium-burning phase. The large applicability of the proposed method to most of the globular clusters in our Galaxy opens the possibility to initiate systematic searches for evolved BSSs, thus giving access to still unexplored phases of their evolution.

Key words: blue stragglers – globular clusters: individual (47 Tucanae) – stars: abundances – techniques: spectroscopic

Supporting material: machine-readable table

1. INTRODUCTION

Blue straggler stars (BSSs) are commonly defined as stars that are brighter and bluer than the main sequence (MS) turn-off point in the color–magnitude diagram (CMD) of the host stellar cluster. They are thought to be central hydrogen-burning stars, more massive than the MS stars (Shara et al. 1997; Gilliland et al. 1998; Fiorentino et al. 2014). Two main processes (able to bring new hydrogen into the core, thus prolonging the MS stage; e.g., Lombardi et al. 1995, 2002; Chen & Han 2009) are currently favored to account for their formation: (1) mass-transfer in binary systems (McCrea 1964), possibly up to the complete coalescence of the two stars (see, however, Preston & Sneden 2000; Carney et al. 2005; Gosnell et al. 2014), and (2) direct stellar collisions (Hills & Day 1976). Both these processes can have an efficiency which depends on the local environment (Fusi Pecci et al. 1992; Ferraro et al. 1993, 2003; Davies et al. 2004; Dalessandro et al. 2008a, 2008b; Knigge et al. 2009), and they can act within the same cluster simultaneously (Ferraro et al. 2009; Xin et al. 2015). Being more massive than the average cluster stars, BSSs suffer from the effect of dynamical friction, which makes them progressively sink toward the cluster center (Mapelli et al. 2006; Lanzoni et al. 2007; Alessandrini et al. 2014) and for this reason they have been found to be powerful probes of the internal dynamical evolution of the host cluster (see Ferraro et al. 2012, 2015; Miocchi et al. 2015).

From the stellar evolution side, these objects are expected to experience all the post-MS evolutionary phases. However, although BSSs have been routinely observed for decades now, in globular clusters, in several open clusters (Geller & Mathieu 2011; Gosnell et al. 2014), and also in dwarf galaxies (Mapelli et al. 2009; Monelli et al. 2012), only a few identifications of evolved BSSs have been obtained so far. Three candidates have been recently identified in two open clusters (NGC 6791 and NGC 6819; Brogaard et al. 2012; Corsaro et al. 2012) from asteroseismology studies. Instead only a possible evolved BSS is known in globular clusters: the anomalous cepheid V19 in NGC 5466 (Zinn & King 1982; McCarthy & Nemec 1997) with an estimated mass of $1.6 M_{\odot}$. Photometric criteria have been suggested to optimize the search for candidate evolved BSSs: for instance, Renzini & Fusi Pecci (1988) and Fusi Pecci et al. (1992) suggested looking at a region of the CMD between the horizontal branch (HB) and the base of the asymptotic giant branch (AGB, the so-called AGB-clump; Ferraro et al. 1999a), where evolved BSSs experiencing the core helium burning phase (predicted to be brighter than *canonical*, lower mass, HB stars) are expected to lie. Following this prescription, statistical evidence based on number counts and radial segregation and pointing to the presence of evolved BSSs "contaminating" the genuine HB-AGB cluster population has been found in M3 (Ferraro et al. 1997), M80 (Ferraro et al. 1999b), and 47 Tucanae (47 Tuc; Beccari et al. 2006).

The identification of evolved BSSs is crucial in the context of BSS formation and evolution models, which currently predict that, at least at first approximation, these objects

* Based on UVES-FLAMES observations collected under Program 193.D-0232.

experience a post-MS evolution analogous to that of any "normal" star of $\sim$1.2–1.6$M_{\odot}$ (Tian et al. 2006; Sills et al. 2009). In fact, the collection of complete samples of these objects in globular clusters (where BSSs and their descendants are expected to be numerous enough) allows the determination of meaningful population ratios from which the characteristic evolutionary timescales can be empirically constrained. Moreover, since evolved BSSs are 20 times more luminous than their progenitors, detailed spectroscopic follow-up studies are largely facilitated. The determination of the chemical abundance patterns of evolved BSSs is further helped by the fact that these stars are cooler (thus providing a larger number of absorption lines) and show slower rotation (hence, sharper lines), with respect to BSSs on the MS, which are hotter and often display significant rotation (see Ferraro et al. 2006; Mathieu & Geller 2009; Lovisi et al. 2010; Mucciarelli et al. 2014).

In this paper we present the results of a high-resolution spectroscopic exploration of three stars located in a region of the CMD slightly brighter than the HB red clump in 47 Tuc. Among them, one object shows chemical properties incompatible with a low-mass object: the iron and titanium abundance measured from ionized lines agrees with that obtained from neutral lines only if a mass of $\sim$1.4$M_{\odot}$ is assumed. The comparison with stellar tracks suggests that this objects is probably a BSS descendant experiencing its helium burning phase.

The paper is organized as follows. The observations, data reduction, and membership determination are discussed in Section 2. The chemical analysis performed on each target and the discussion of its uncertainties are presented in Section 3. Section 4 is devoted to the discussion of the obtained results in the context of BSS evolution. Section 5 summarizes the results and conclusions of the work.

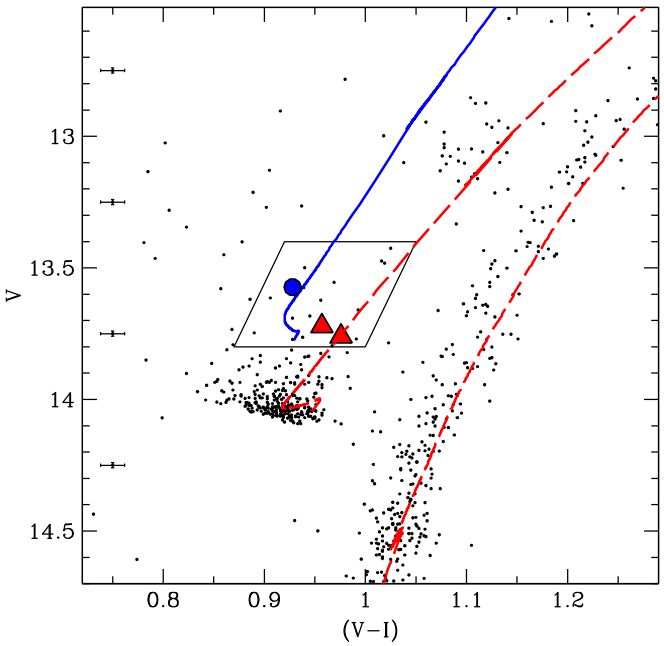

Figure 1. Magnified portion of the (V, $V-I$) CMD of 47 Tuc around the horizontal branch. The large blue circle marks the position of E-BSS1. The position of the two reference targets (bHB1 and bHB2) are marked with red triangles. For reference, only stars within 50″ from the center are plotted (small black dots). Error bars are marked at different magnitude levels. The red dashed line corresponds to the evolutionary track (Pietrinferni et al. 2006) of a single star of 0.9$M_{\odot}$ well reproducing the cluster main evolutionary sequences. The evolutionary track, from the HB to the AGB, for a star with a MS mass of 1.5 $M_{\odot}$ is also shown (blue solid line). Because of mass loss during the red giant branch, the stellar mass at the HB level for this evolutionary track is $\sim$1.4$M_{\odot}$, well in agreement with the spectroscopic estimate for E-BSS1. The marked box delimitates the region where evolved BSSs experiencing the HB stage are expected to lie: the blue and red boundaries of the box are approximately set by the tracks corresponding to MS turn-off masses of 1.8 $M_{\odot}$ and 0.9 $M_{\odot}$, respectively.

2. OBSERVATIONS AND MEMBERSHIP

In the context of the ESO Large Programme 193.D-0232 (PI: Ferraro) aimed at studying the internal kinematics of Galactic globular clusters, we have secured UVES-FLAMES (Pasquini et al. 2000) high-resolution spectra of three stars in 47 Tuc. The targets (hereafter named bHB1, bHB2, and E-BSS1). have been selected in a region of the CMD slightly brighter than the red clump (see Figure 1), where evolved BSSs experiencing the core helium burning process are expected to lie (see also Beccari et al. 2006). All the targets lie within a distance of $\sim$132″ from the cluster center, corresponding to 4.5 r_c or 0.6 $r_{\rm hm}$ ($r_c = 29''$ and $r_{\rm hm} = 213''$ being, respectively, the core and half-mass radii of 47 Tuc; Miocchi et al. 2013). Figure 1 shows the (V, $V-I$) CMD obtained from the *Hubble Space Telescope* (*HST*)-Advanced Camera for Surveys (ACS) photometric catalog of Sarajedini et al. (2007), with the target selection box marked. The color and magnitude of bHB2 (which is located beyond the ACS field of view) are from ground-based wide field data (Ferraro et al. 2004) homogenized to the Johnson-Cousin photometric system. The coordinates, V band magnitude, $V-I$ color, and distance from the center of each target are listed in Table 1.

The target spectra have been acquired with the grating 580 Red Arm CD#3, which provides a spectral resolution $R \sim 40{,}000$ between 4800 and 6800 Å. All the spectra have been reduced by using the dedicated ESO pipeline, performing bias subtraction, flat-fielding, wavelength calibration, and order merging. During the observations, a number of fibers were allocated on empty regions to sample the sky background, which has then been subtracted from the target spectra. The total exposure time is $\sim$30 minutes for each star, providing a signal-to-noise ratio (S/N) $\geqslant$ 50 per pixel.

The three stars are all cluster members, as assessed by their radial velocity (see Table 1) and the systemic velocity and velocity dispersion of 47 Tuc ($V_r = -17.6\,{\rm km\,s^{-1}}$ and $\sigma = 11.5\,{\rm km\,s^{-1}}$, respectively, from Lapenna et al. 2014; see also Carretta et al. 2004; Alves-Brito et al. 2005; Ferraro et al. 2006; Koch & McWilliam 2008; Lane et al. 2010; Gratton et al. 2013; Cordero et al. 2014; Thygesen et al. 2014; Johnson et al. 2015). The radial velocities have been determined with the code DAOSPEC (Stetson & Pancino 2008), by measuring the position of up to 300 metallic lines. The final uncertainty was obtained by dividing the dispersion of the velocities by the square root of the number of lines used.

Unfortunately no proper motion measures are available for such bright stars (A. Bellini 2015, private communication). To further check the possible contamination by field stars, we extracted the distribution of radial velocities and metallicities of a sample of about 1700 field objects from the the Besançon Galactic model (Robin et al. 2003). We found that no field stars are present in the CMD region corresponding to the position of the targets and with radial velocities and metallicities similar to those of 47 Tuc. We can also safely exclude a contamination

Table 1
Observational Parameters of the Three Targets

Name	ID	R.A. (J2000)	decl. (J2000)	V	$(V-I)$	r (arcsec)	$T_{\rm eff}$ (K)	V_r (km s^{-1})
E-BSS1	1090214	6.0601164	−72.0726528	13.573	0.928	50.6	5013	−24.3 ± 0.05
bHB1	1109049	6.0001040	−72.0720222	13.761	0.976	42.1	4896	−7.8 ± 0.06
bHB2	2625792	5.9343037	−72.1054776	13.722	0.957	132.2	4940	−11.7 ± 0.06

Note. Coordinates, V band magnitude, $(V-I)$ color, distance from the center, effective temperature, and radial velocity of the three target stars. The cluster center used to compute the distance from the center is from Miocchi et al. (2013).

from stars belonging to the Small Magellanic Cloud (SMC), since the brightest SMC objects (at the red giant branch tip) are located at much fainter magnitudes ($V \sim 16.5$ mag) and have quite different radial velocities (between +50 and +250 km s^{-1}; Harris & Zaritsky 2006).

3. CHEMICAL ANALYSIS

The chemical analysis has been performed following the same approach already used in Lapenna et al. (2014). The equivalent widths (EW) and the relative uncertainty have been measured with DAOSPEC, iteratively launched by the 4DAO[4] code (Mucciarelli 2013). Abundances were obtained with the code GALA[5] (Mucciarelli et al. 2013) by matching the measured and theoretical EWs and adopting the ATLAS9 model atmospheres and the solar values of Grevesse & Sauval (1998). To avoid saturated or too weak features, we have used only the lines with reduced EWs[6] ranging between −5.6 and −4.5 and we have discarded those with EW uncertainties larger than 20%. The computation of the final iron abundances has been performed by using up to 127 Fe I lines and 9 Fe II lines. To derive the abundances of titanium we exploited 20 Ti I lines and 11 Ti II lines. All the three targets have been analyzed using the same line list, which is provided in Table 2.

The microturbulence velocity (see Table 3) has been optimized spectroscopically by requiring that no trends exist between the abundance derived from Fe I lines and the reduced EWs. To determine the stellar surface gravity ($\log g$) an estimate of the stellar mass and radius is needed. The latter is obtained from the Stefan–Boltzmann equation once the surface temperature (see Table 1) has been determined from the $(V-I)_0$ color–temperature relation of Alonso et al. (1999), after transforming the Johnson-Cousin $(V-I)_0$ color into the Johnson system following appropriate transformations (Bessell 1979). The stellar luminosity has been evaluated by projecting the CMD position of each star onto the best-fit isochrone (from Pietrinferni et al. 2006) and assuming a distance of 4.45 kpc and a color excess $E(B-V) = 0.04$ (see Harris 1996). As for the stellar mass, which value is expected for the three targets? Due to the mass-loss occurring along the red giant branch, stars evolving on the HB are expected to be less massive than MS turn-off stars by $\sim 0.1 - 0.15 M_{\odot}$ (Renzini & Fusi Pecci 1988; Origlia et al. 2007, 2010, 2014). Recently, Gratton et al. (2010) derived the mass distribution of HB stars in several globular clusters, obtaining values between ~ 0.6 and $0.7 M_{\odot}$ in the case of 47 Tuc. These values are 0.1–0.2 $M_{\odot}$ lower than the turn-off mass of the best-fit isochrone ($0.85 M_{\odot}$), in full agreement with the expected amount of mass-loss during the red giant branch. Adopting a mass of $0.6 M_{\odot}$ and the photometric measure of the effective temperature, we obtained surface gravities of ∼2.0 and we derived the Fe I and Fe II abundances of the three targets (see Table 3).

Table 2
Adopted Line List

Wavelength (Å)	El.	E.P. (eV)	log gf	EW$_{\rm E\text{-}BSS1}$ (mA)	EW$_{\rm bHB1}$ (mA)	EW$_{\rm bHB2}$ (mA)
4834.507	Fe I	2.42	−3.330	29.50	39.10	0.00
4841.785	Fe I	4.19	−1.880	0.00	15.70	0.00
4877.606	Fe I	3.00	−3.090	0.00	16.20	0.00
4885.430	Fe I	3.88	−1.095	63.60	66.40	61.40
4896.439	Fe I	3.88	−2.020	0.00	23.40	20.30
4909.383	Fe I	3.93	−1.327	54.60	57.70	52.90
4917.230	Fe I	4.19	−1.160	51.70	52.10	47.70
4918.013	Fe I	4.23	−1.340	35.80	38.20	39.60
4924.770	Fe I	2.28	−2.114	92.90	107.50	98.70

Note. Columns 1 to 6 provide: wavelength, element, excitation potential, oscillator strength, and equivalent width of adopted lines.

(This table is available in its entirety in machine-readable form.)

For all the targets we found values of [Fe I/H] in agreement with the mean metallicity of 47 Tuc ([Fe/H] = −0.83 dex, $\sigma = 0.03$ dex; Lapenna et al. 2014). This suggests that the target stars are not affected by departures from local thermal equilibrium (LTE)[7] and the abundance derived from Fe I lines is a reliable measure of the iron content of the stars. However, only for two objects (namely bHB1 and bHB2) does the value of the iron abundance obtained from the ionized lines (Fe II) agree, within 0.01 dex, with that derived from Fe I, while it is sensibly (∼0.2 dex) lower for E-BSS1. This is the opposite of what is predicted and observed in the case of departures from LTE conditions, while it could be explained as an effect of surface gravity and, hence, of stellar mass. In fact the absorption lines of ionized elements are sensitive to changes in surface gravity, while neutral lines are not. This is due to the fact that, in the case of highly ionized elements (like Fe), the line-to-continuous opacity ratio of the neutral lines is independent of pressure (i.e., gravity), while it shows a dependence in ionized lines (see Gray 1992). Taking this into account, we evaluated the effect of increasing the stellar mass by re-performing the spectral analysis for different values of the surface gravity.

[4] http://www.cosmic-lab.eu/4dao/4dao.php
[5] http://www.cosmic-lab.eu/gala/gala.php
[6] Reduced EWs are defined as $\log(EW/\lambda)$, with λ being the wavelength.
[7] In fact, departures from LTE conditions affect the minority species, leading to an under-estimate of [Fe I/H], while they have no impact on the abundances obtained from the dominant species, as single ionized iron lines (see also Ivans et al. 2001; Mashonkina et al. 2011; Mucciarelli et al. 2015).

Table 3
Abundance Ratios of Fe and Ti Obtained by Adopting Different Stellar Mass (Gravity) Values

Mass ($M_\odot$)	log g^{phot} (dex)	v_{turb}^{spec} (km s^{-1})	[Fe I/H] (dex)	n(Fe I)	[Fe II/H] (dex)	n(Fe II)	[Ti I/H] (dex)	n(Ti I)	[Ti II/H] (dex)	n(Ti II)
					E-BSS1					
0.60	2.03	1.30	−0.79 ± 0.01	122	−0.97 ± 0.01	9	−0.56 ± 0.01	21	−0.76 ± 0.05	11
0.70	2.10	1.25	−0.77 ± 0.01	122	−0.92 ± 0.01	9	−0.57 ± 0.01	20	−0.73 ± 0.05	11
0.80	2.15	1.25	−0.78 ± 0.01	121	−0.90 ± 0.01	9	−0.57 ± 0.01	20	−0.71 ± 0.05	11
0.90	2.21	1.25	−0.78 ± 0.01	121	−0.87 ± 0.01	9	−0.57 ± 0.01	20	−0.68 ± 0.05	11
1.00	2.25	1.20	−0.76 ± 0.01	123	−0.84 ± 0.01	9	−0.57 ± 0.01	20	−0.66 ± 0.05	11
1.10	2.30	1.20	−0.76 ± 0.01	123	−0.82 ± 0.01	9	−0.57 ± 0.01	21	−0.63 ± 0.05	11
1.20	2.33	1.20	−0.77 ± 0.01	122	−0.80 ± 0.01	9	−0.57 ± 0.01	21	−0.62 ± 0.05	11
1.30	2.37	1.20	−0.77 ± 0.01	125	−0.79 ± 0.01	9	−0.57 ± 0.01	21	−0.61 ± 0.05	11
1.40	2.40	1.15	−0.76 ± 0.01	127	−0.76 ± 0.01	9	−0.57 ± 0.01	20	−0.59 ± 0.05	11
					bHB1					
0.60	2.06	1.35	−0.84 ± 0.01	129	−0.85 ± 0.01	12	−0.66 ± 0.01	26	−0.69 ± 0.05	14
0.70	2.13	1.35	−0.84 ± 0.01	128	−0.82 ± 0.01	12	−0.66 ± 0.01	26	−0.66 ± 0.05	14
0.80	2.18	1.35	−0.84 ± 0.01	128	−0.80 ± 0.01	12	−0.66 ± 0.01	26	−0.64 ± 0.05	14
0.90	2.23	1.35	−0.84 ± 0.01	127	−0.78 ± 0.01	12	−0.66 ± 0.01	26	−0.62 ± 0.05	14
1.00	2.28	1.35	−0.84 ± 0.01	126	−0.75 ± 0.01	12	−0.66 ± 0.01	26	−0.59 ± 0.05	14
1.10	2.32	1.35	−0.84 ± 0.01	126	−0.73 ± 0.01	12	−0.66 ± 0.01	26	−0.58 ± 0.05	14
1.20	2.36	1.35	−0.84 ± 0.01	126	−0.72 ± 0.01	12	−0.67 ± 0.01	26	−0.57 ± 0.05	14
1.30	2.39	1.30	−0.83 ± 0.01	126	−0.69 ± 0.01	12	−0.67 ± 0.01	26	−0.55 ± 0.05	14
1.40	2.43	1.30	−0.83 ± 0.01	127	−0.67 ± 0.01	12	−0.67 ± 0.01	26	−0.54 ± 0.05	14
					bHB2					
0.60	2.06	1.20	−0.81 ± 0.01	124	−0.81 ± 0.02	10	−0.68 ± 0.01	22	−0.67 ± 0.05	13
0.70	2.13	1.20	−0.81 ± 0.01	128	−0.78 ± 0.02	10	−0.68 ± 0.01	22	−0.64 ± 0.05	13
0.80	2.19	1.20	−0.82 ± 0.01	129	−0.75 ± 0.02	10	−0.68 ± 0.01	22	−0.61 ± 0.05	13
0.90	2.24	1.15	−0.80 ± 0.01	128	−0.72 ± 0.02	11	−0.68 ± 0.01	22	−0.59 ± 0.05	13
1.00	2.29	1.15	−0.78 ± 0.01	127	−0.68 ± 0.02	11	−0.68 ± 0.01	22	−0.57 ± 0.05	13
1.10	2.33	1.15	−0.80 ± 0.01	125	−0.68 ± 0.02	11	−0.68 ± 0.01	22	−0.56 ± 0.05	13
1.20	2.37	1.10	−0.79 ± 0.01	125	−0.65 ± 0.02	11	−0.68 ± 0.01	22	−0.54 ± 0.05	13
1.30	2.40	1.10	−0.78 ± 0.01	124	−0.63 ± 0.02	11	−0.69 ± 0.01	22	−0.53 ± 0.05	13
1.40	2.43	1.10	−0.79 ± 0.01	124	−0.62 ± 0.02	11	−0.69 ± 0.01	22	−0.52 ± 0.05	13

Note. Iron and titanium abundance ratios obtained for the program stars by adopting the mass values listed in the first column. During the analysis the effective temperature (listed in Table 1) and surface gravity (column 2) have been kept fixed, while the microturbulent velocity (column 3) has been spectroscopically optimized. The abundances obtained from neutral and ionized lines, and the number of lines used are listed in columns 4–11 (see the labels). We adopted the solar reference values of Grevesse & Sauval (1998).

In Table 3 we list the values of [Fe I/H] and [Fe II/H] obtained by varying the star mass in steps of $0.1M_\odot$ while keeping the effective temperature fixed. The upper panel of Figure 2 shows the resulting behavior. As expected, in all cases the Fe I abundance remains essentially unaltered (and consistent with the cluster metallicity), while [Fe II/H] systematically increases for increasing mass (gravity). The behavior of the difference between Fe II and Fe I abundances as a function of the adopted stellar mass is plotted in the left panels of Figure 3 for the three targets. Clearly, while for two stars (bHB1 and bHB2) a good agreement between the Fe I and Fe II abundances is reached at 0.6 $M_\odot$, for E-BSS1 a significantly larger stellar mass (1.3–1.4 $M_\odot$, corresponding to a gravity $\log g = 2.4$ dex) is needed. Thus, a mass larger than twice the mass expected for a canonical post-HB cluster star is needed in order to reconcile the Fe I and Fe II abundances of E-BSS1. Conversely, the difference [Fe II/H]–[Fe I/H] for the other two targets tends to diverge for increasing stellar mass (see Figure 3), indicating that the adopted values of the surface gravity become progressively unreasonable.

As a double check, the same procedure has been performed on the titanium lines, since this is one of the few other elements providing large numbers of both neutral and single ionized lines. Also in this case, the same abundance of Ti I and Ti II is reached, within the errors, only if a mass of 1.4 $M_\odot$ is adopted for E-BSS1, while the best agreement is reached at 0.6–0.7 $M_\odot$ for bHB1 and bHB2 (see the right panels of Figure 3). This fully confirms the results obtained from the iron abundance analysis, pointing out that E-BSS1 is an object significantly more massive than the others.

Additional support comes from the inspection of another feature that is known to be sensitive to the stellar surface gravity: the wings of the Mg I b triplet at 5167.3, 5172.6, and 5183.6 Å. In fact, these lines are located in the damped part of the curve of growth, where the line broadening, occurring mainly on the wings, is driven by the collisions between atoms and other particles (the so-called pressure broadening). In Figure 4 we show a comparison between the observed spectrum of E-BSS1 and two synthetic spectra computed by assuming the atmospheric parameters listed in Table 1 and the measured Mg abundance; only the surface gravity has been

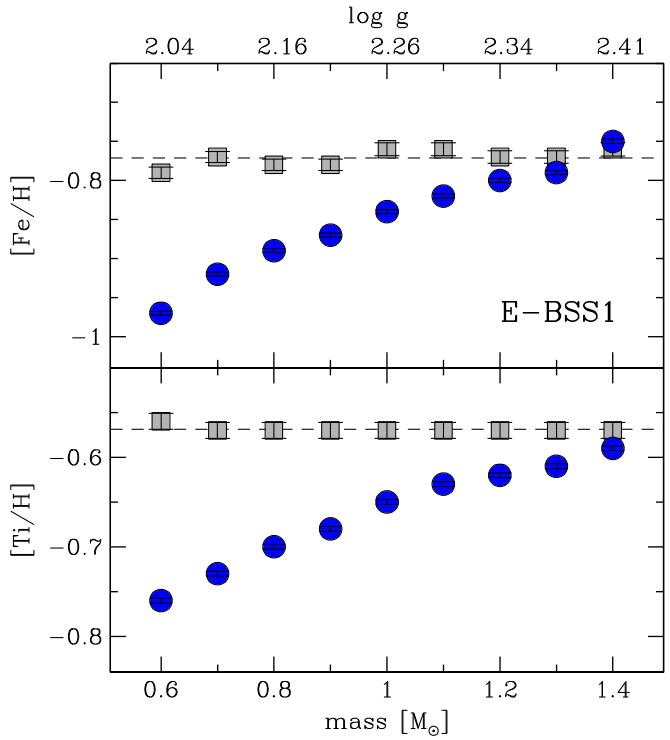

Figure 2. Top panel: iron abundance of E-BSS1 derived from Fe I lines (gray squares) and Fe II lines (blue circles), as a function of the assumed stellar mass. Errors in the derived abundances are smaller than the symbol sizes. The dashed line marks the average Fe I abundance (corresponding well to the metallicity of 47 Tuc: [Fe/H] = −0.83 dex; e.g., Lapenna et al. 2014). In the top axis of the panel, the logarithmic values of the stellar surface gravity corresponding to the various adopted masses are labeled. Bottom panel: same as the top panel, but for the Ti abundance, as derived from Ti I lines (gray squares) and Ti II lines (blue circles).

varied: we adopted $\log g = 2.03$ and $\log g = 2.40$ dex (corresponding to 0.6 and 1.4 $M_{\odot}$, respectively). Clearly, the synthetic spectrum computed for $\log g = 2.03$ dex fails to fit the wings of the Mg I b triplet, while that computed assuming a $1.4M_{\odot}$ stellar mass closely reproduces the observed spectrum. All these findings point out that E-BSS1 is an object significantly more massive than the other targets and canonical cluster stars.

3.1. Uncertanties

It is worth noting that, in doing the comparison between the abundances derived from the ionized and the neutral species, we performed a differential analysis, with the most critical parameters (as temperature, microturbulence and gravity) set to the same value. Hence only internal errors, due to the quality of the spectra and the number of the absorption lines used, need to be considered, while potential external sources of errors can be neglected.

The global uncertainty on the difference between ionized and neutral chemical abundances has been determined by taking into account the effect of atmospheric parameter variations and the covariance terms due to their correlations (Cayrel et al. 2004). We estimate that the global effect of varying the temperature by 40 K (corresponding to an error in color of the order of 0.015 mag) produces a variation of 0.01 dex on the abundance difference. By adding in quadrature this term with the uncertainties due to the EW measurements (which are of the order of 0.01 dex for both the abundance ratios), we estimate a total error of about 0.02 dex on the derived abundance differences.

We emphasize that the only way to make the Fe II abundance in agreement with that of Fe I, while simultaneously complying with the other constraints, is to assume a large mass (gravity) for E-BSS1. In fact, departures from LTE conditions would affect the neutral species (yielding to an under-estimate of [Fe I/H]), leaving the abundances obtained from single ionized lines (Ivans et al. 2001; Mashonkina et al. 2011; Mucciarelli et al. 2015) unaltered. The micro-turbulence velocity has a negligible impact on the derived abundances, and its effect is the same (both in terms of absolute value and direction) on the abundances derived from neutral and from ionized lines: hence, it cannot help reconciling the value of [Fe II/H] with that of [Fe I/H]. Finally, if for E-BSS1 we assume a mass sensibly lower than 1.4 $M_{\odot}$ (for instance 0.6–0.8 $M_{\odot}$, as appropriate for HB and giant stars in 47 Tuc), Fe II would agree with Fe I only if the effective temperature is lowered by ∼130 K. However, this solution is not acceptable because it implies a non-zero slope between the iron abundance and the excitation potential. Moreover, such a low value of $T_{\rm eff}$ corresponds to a photometric color that is completely inconsistent with the observed one (note the internal accuracy of the *HST* photometry for such a bright object is less than 0.01 mag). Thus, the spectra inevitably lead to the conclusion that E-BSS1 is significantly more massive than the other stars.

4. DISCUSSION

Indeed the mass derived for E-BSS1 ($1.4M_{\odot}$) is by far too large for a genuine HB cluster star evolving toward the AGB (the MS turn-off mass in 47 Tuc is 0.85 $M_{\odot}$; see Section 3). Moreover, the mass values that we obtained for targets bHB1 and bHB2 from our analysis turn out to be fully in agreement with the values (0.6–0.7 $M_{\odot}$) recently estimated for typical HB stars in 47 Tuc (Gratton et al. 2010). Notably, these are also the values that we obtained for targets bHB1 and bHB2 from our analysis. These results clearly demonstrate that the detailed comparison between neutral and ionized chemical abundances is a powerful *weighing device* able to reliably determine stellar masses in a self-consistent and differential way (this is quite relevant since it gets rid of any possible zero-point offset among different methods).

If E-BSS1 were coeval to the other low-mass stars populating the cluster, such a massive object would have already evolved into a white dwarf several Gyr ago. The only possibility is that it formed more recently, through a mass-enhancement process: it could therefore be the descendant of a BSS. As any other star, BSSs are then expected to evolve along the various post-MS phases. Indeed, E-BSS1 is located in the region of the CMD where evolved BSSs experiencing the core helium burning process are expected to lie. In fact, the collisional models of Sills et al. (2009) show that, during the core helium burning stage, the progeny of collisional BSSs should populate the CMD slightly blueward of the red giant branch, between 0.2 and 1 mag brighter than the "canonical" HB level of the host cluster.[8] Overall, the post-MS evolution of

[8] Unfortunately no specific tracks for the post-MS evolution of mass-transfer BSSs in globular clusters are available at the moment. However, the models specifically built for the open cluster M67 (Tian et al. 2006) and the globular cluster M30 (Xin et al. 2015) suggest that, after mass-transfer, BSSs behave largely as normal single stars of comparable mass. Hence they are also expected to populate the same region of the CMD.

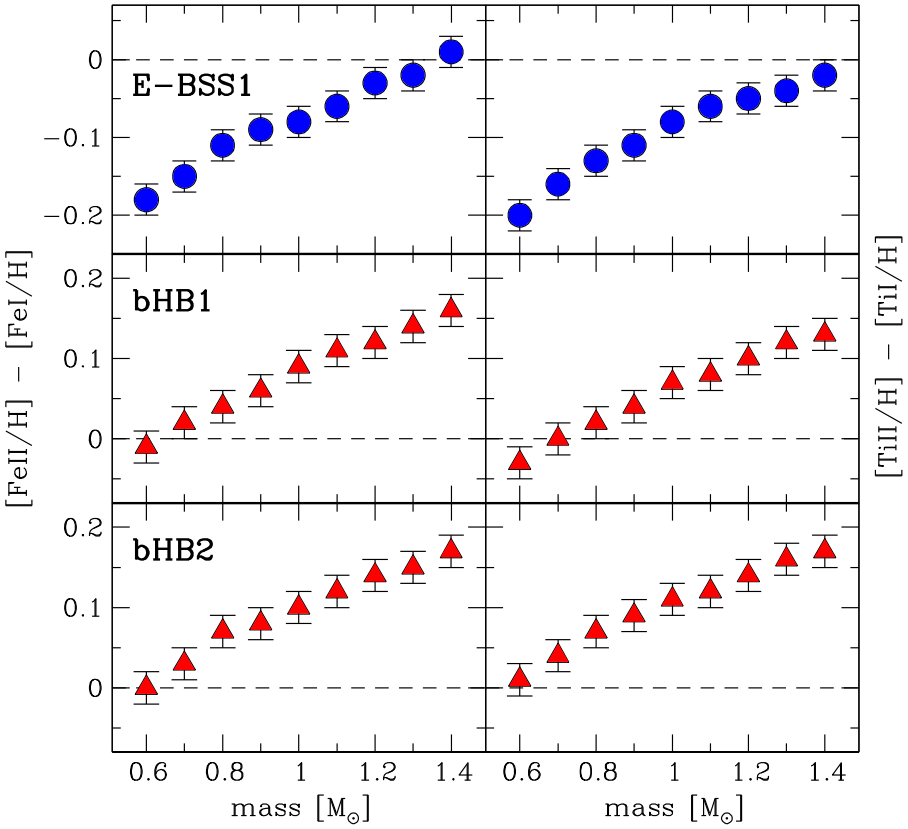

Figure 3. Top panel: difference between the iron abundances derived from ionized lines and that obtained from neutral lines, as a function of the assumed stellar mass (left-hand panel) for E-BSS1. The same, but for the titanium abundances, is shown in the right-hand panels. Mid panel: same as in the top panel, but for target bHB1. Bottom panel: same as in the top panel, but for target bHB2.

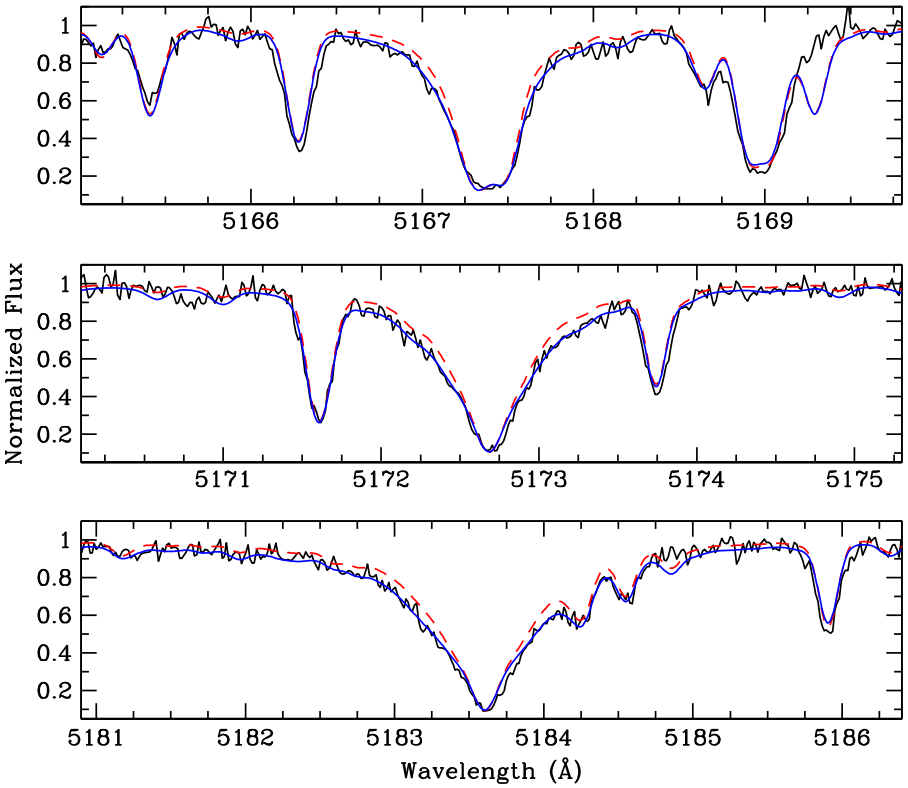

Figure 4. Comparison between the observed spectrum (solid black line) and two synthetic spectra for the Mg I lines at 5167.3, 5172.6 and 5183.6 Å. The synthetic spectra have been computed by adopting $T_{\rm eff} = 5013$ K and $v_{\rm turb} = 1.20$ km s^{-1} and by adopting two different values of the surface gravity: $\log g = 2.03$ dex corresponding to a stellar mass of $0.6M_{\odot}$ (dashed red line) and $\log g = 2.40$ dex corresponding to $1.4M_{\odot}$ (solid blue line). Clearly, the spectrum obtained for a $0.6M_{\odot}$ star is unable to reproduce the observations, while the observed wings of the Mg I b triplet are very well matched under the assumption of a $1.4M_{\odot}$ stellar mass.

a collisional product in the CMD is very similar to that of a normal star of the same mass, the former being just a few tens of degree hotter (see Figure 6 of Sills et al. 2009 for the model of a $\sim 1.4 M_{\odot}$ star). In the following analysis, we therefore adopted "normal" evolutionary tracks. In Figure 1 we have superimposed to the CMD of 47 Tuc the evolutionary track (from Pietrinferni et al. 2006) of a star with initial mass equal to $1.5 M_{\odot}$ (reaching the HB phase with a mass of $1.4 M_{\odot}$). We note that E-BSS1 lies in a region very close to the red clump level of this track, corresponding to an effective temperature $T_{\rm eff} \simeq 5011$ K and a surface gravity $\log g \sim 2.47$ dex. These values are in very good agreement with those derived from the chemical analysis of this object. It therefore seems perfectly reasonable to identify our star with an evolved BSS that is currently experiencing its red clump (core helium burning) phase before ascending the AGB.

How rare are evolved BSSs? The number of evolved BSSs observable along the HB stage is predicted to be small even in a massive cluster like 47 Tuc. An estimate can be derived by combining the theoretical ratio between the characteristic MS and HB lifetimes, with the observed number of BSSs. In fact, the observational survey of (Ferraro et al. 2004) counted 110 BSSs over the entire cluster extension, with approximately 40% of the population being segregated within two core radii ($r < 50''$) from the center, which is the distance where E-BSS1 is located. However, this survey sampled only on the brightest portion of the population and deep UV observations sampling the entire BSS sequence (Ferraro et al. 2001) indicate that the total population is $\sim$1.7 times larger. Based on these numbers, it is reasonable to expect $\sim$75 BSSs within $r < 50''$.

On the other hand, evolutionary tracks of collisional BSSs (Sills et al. 2009) show that the HB lifetime is approximately constant ($\sim 10^8$ years, similar to the HB duration for low-mass single stars), regardless of the original stellar masses at the time of the collision. Instead the MS lifetime of collisional BSSs can change by two orders of magnitude.[9] Thus, the predicted number of BSSs in the HB evolutionary stage sensibly depends on the mass of the BSS progenitor. For instance, for a $1.4 M_{\odot}$ BSS originated from the collision of a $0.8 + 0.6 M_{\odot}$ pair, Sills et al. (2009) predict $t_{\rm MS} = 0.82$ Gyr and $t_{\rm HB} = 0.096$ Gyr, thus yielding $t_{\rm MS}/t_{\rm HB} = 8.5$, while this ratios turns out to be 17.7 on average. By considering these two values as reasonable extremes for the ratio $t_{\rm MS}/t_{\rm HB}$, we expect to observe 4–9 evolved BSSs experiencing the helium burning phase out of a total population of 75 BSSs (in the MS stage).

Note that in the same region of the cluster ($r < 50''$), several hundred genuine low-mass stars, with quite similar photometric properties and experiencing the same evolutionary phase, are observed. However, because of their larger mass, evolved BSSs in the HB stage are expected to appear brighter than "normal" low-mass HB stars and to lie along the path of low-mass stars evolving toward the AGB. For genuine low-mass stars the transition from the HB to the AGB phase (see the box in Figure 1) is quite rapid: $\sim$3.5 million years, corresponding to approximately 4% of the time they spent in the HB phase. Based on these considerations and the fact that within $50''$ from the cluster center we count 270 objects in the HB clump, we would have expected to observe $\sim$11 stars within the box drawn in Figure 1. Instead 20 stars are counted. According to these estimates, roughly half of the stars within $50''$ from the cluster center and lying in the selection box could be evolved BSSs. Hence beside E-BSS1, eight additional stars in the box could be evolved BSSs. This is in very good agreement with the prediction above, based on the number of BSSs observed on the MS. It is also consistent with previous evidence (Beccari et al. 2006) showing that the radial distribution of supra-HB stars in 47 Tuc is anomalously segregated in the center, as expected if a significant fraction of them is made of objects heavier than the average, sunk to the bottom of the potential well because of the cluster dynamical evolution (Ferraro et al. 2012).

[9] Note that, from the comparison between Tables 2 and 3 in Sills et al. (2009), the MS lifetime of collisional products turn out to be 40%–70% smaller than that of a normal single star with similar mass.

5. SUMMARY AND CONCLUSIONS

In this work we have performed a chemical analysis of three stars observed between the HB and the AGB regions in the CMD of the Galactic globular cluster 47 Tuc. By using high-resolution spectra acquired at the Very Large Telescope, we have used the difference between iron and titanium abundances derived from neutral and ionized lines as a *weighing device* to derive the stellar mass. This provided convincing evidence that one target (E-BSS1) is significantly more massive ($\sim 1.4 M_{\odot}$) than normal cluster stars, while the other two targets (bHB1 and bHB2) have masses of 0.6–0.7 $M_{\odot}$, perfectly consistent with the theoretical expectations. These results clearly demonstrate that the detailed comparison between neutral and ionized chemical abundances is a powerful *weighing device* able to reliably determine stellar masses in a self-consistent and differential way. The presence of such a high-mass star in that region of the CMD strongly suggests that it is an evolved descendant of a BSS, caught during its core He-burning phase. Interestingly, the ratio between the characteristic MS and HB evolutionary times and the number of BSSs observed in 47 Tuc suggests that a few other evolved BSSs should populate the same region of the CMD.

The proposed *weighing device*, by efficiently pinpointing (heavy) evolved BSSs into the dominant and photometrically indistinguishable population of genuine (low-mass) stars, opens the route to systematic searches of evolved BSSs in globular clusters, thus allowing detailed spectroscopic follow-up studies with the concrete possibility to even go back to the formation channel. In fact, a few characterizing features impressed by the formation process could still be observable in such advanced stages of the evolution. One of the most solid predictions of the mass-transfer scenario is that mass-transfer BSSs should be bound in a binary system with a compact (degenerate) companion star (the peeled core of the donor, probably a helium white dwarf). This was recently confirmed in the open cluster NGC 188 (Gosnell et al. 2014). Thanks to the high luminosity of evolved BSSs, spectroscopic follow-up observations would make such a prediction easily testable through the measurement of periodic radial velocity variations. Since no companion is expected in the collisional scenario (which ends up with the merger of the two progenitors), this kind of study is particularly important in globular clusters, where both formation channels are expected to be active but their relative efficiency is still unknown. Moreover, detailed spectroscopic follow-ups providing the entire chemical pattern of evolved BSSs represent an additional and highly fruitful route toward the full characterization of their evolution. In fact, significant depletion of chemical species like carbon and oxygen has been observed in a sub-sample of BSSs in 47 Tuc

and it has been interpreted as the chemical signature of the mass-transfer origin of these objects (Ferraro et al. 2006). However, it is still unknown whether this signature is transient and on which timescales. Hence, any additional information obtained from more advanced stages of the evolution can provide new clues about the degree of mixing experienced by these stars. Indeed, after the detection of E-BSS1, the proposed *weighing device* promises to boost the identifications of evolved BSSs, thus providing unprecedented constraints to the theoretical modeling of these exotica and opening a new perspective on the comprehension of their evolutionary paths and formation processes.

This paper is dedicated to Prof. Flavio Fusi Pecci, one of the first scientists indicating the route to search for evolved BSSs in GCs: his pioneering work has inspired our research over the years. We thank the referees for useful comments that improved the paper's presentation. This research is part of the project *Cosmic-Lab* (see http://www.cosmic-lab.eu) funded by the European Research Council (under contract ERC-2010-AdG-267675). E.L. acknowledges the *Marco Polo* program for grant support and the Institute for Astronomy, University of Edinburgh & STFC (U.K.), for the hospitality during the period when most of this work was carried out.

REFERENCES

Alessandrini, E., Lanzoni, B., Miocchi, P., Ciotti, L., & Ferraro, F. R. 2014, ApJ, 795, 169
Alonso, A., Arribas, S., & Martínez-Roger, C. 1999, A&AS, 140, 261
Alves-Brito, A., Barbuy, B., Ortolani, S., et al. 2005, A&A, 435, 657
Beccari, G., Ferraro, F. R., Lanzoni, B., & Bellazzini, M. 2006, ApJL, 652, L121
Bessell, M. S. 1979, PASP, 91, 589
Brogaard, K., VandenBerg, D. A., Bruntt, H., et al. 2012, A&A, 543, AA106
Carney, B. W., Latham, D. W., & Laird, J. B. 2005, AJ, 129, 466
Carretta, E., Gratton, R. G., Bragaglia, A., Bonifacio, P., & Pasquini, L. 2004, A&A, 416, 925
Cayrel, R., Depagne, E., Spite, M., et al. 2004, A&A, 416, 1117
Chen, X. F., & Han, Z. W. 2009, MNRAS, 395, 1822
Cordero, M. J., Pilachowski, C. A., Johnson, C. I., et al. 2014, ApJ, 780, 94
Corsaro, E., Stello, D., Huber, D., et al. 2012, ApJ, 757, 190
Dalessandro, E., Lanzoni, B., Ferraro, F. R., et al. 2008a, ApJ, 681, 311
Dalessandro, E., Lanzoni, B., Ferraro, F. R., et al. 2008b, ApJ, 677, 1069
Davies, M. B., Piotto, G., & de Angeli, F. 2004, MNRAS, 349, 129
Ferraro, F. R., Beccari, G., Dalessandro, E., et al. 2009, Natur, 462, 1028
Ferraro, F. R., Beccari, G., Rood, R. T., et al. 2004, ApJ, 603, 127
Ferraro, F. R., D'Amico, N., Possenti, A., Mignani, R. P., & Paltrinieri, B. 2001, ApJ, 561, 337
Ferraro, F. R., Lanzoni, B., Dalessandro, E., Mucciarelli, A., & Lovisi, L. 2015, in Ecology of Blue Straggler Stars, ed. H. M. J. Boffin, G. Carraro, & G. Beccari (Berlin: Springer-Verlag), 99
Ferraro, F. R., Lanzoni, B., Dalessandro, E., et al. 2012, Natur, 492, 393
Ferraro, F. R., Messineo, M., Fusi Pecci, F., et al. 1999a, AJ, 118, 1738
Ferraro, F. R., Paltrinieri, B., Fusi Pecci, F., et al. 1997, A&A, 324, 915
Ferraro, F. R., Paltrinieri, B., Rood, R. T., & Dorman, B. 1999b, ApJ, 522, 983
Ferraro, F. R., Pecci, F. F., Cacciari, C., et al. 1993, AJ, 106, 2324
Ferraro, F. R., Sabbi, E., Gratton, R., et al. 2006, ApJL, 647, L53
Ferraro, F. R., Sills, A., Rood, R. T., Paltrinieri, B., & Buonanno, R. 2003, ApJ, 588, 464
Fiorentino, G., Lanzoni, B., Dalessandro, E., et al. 2014, ApJ, 783, 34
Fusi Pecci, F., Ferraro, F. R., Corsi, C. E., Cacciari, C., & Buonanno, R. 1992, AJ, 104, 1831
Geller, A. M., & Mathieu, R. D. 2011, Natur, 478, 356
Gilliland, R. L., Bono, G., Edmonds, P. D., et al. 1998, ApJ, 507, 818
Gosnell, N. M., Mathieu, R. D., Geller, A. M., et al. 2014, ApJL, 783, LL8
Gratton, R. G., Carretta, E., Bragaglia, A., Lucatello, S., & D'Orazi, V. 2010, A&A, 517, AA81
Gratton, R. G., Lucatello, S., Sollima, A., et al. 2013, A&A, 549, AA41
Gray, D. F. 1992, The Observation and Analysis of stellar Photospheres (Cambridge: Cambridge Univ. Press), 374
Grevesse, N., & Sauval, A. J. 1998, SSRv, 85, 161
Harris, J., & Zaritsky, D. 2006, AJ, 131, 2514
Harris, W. E. 1996, AJ, 112, 1487
Hills, J. G., & Day, C. A. 1976, ApL, 17, 87
Ivans, I. I., Kraft, R. P., Sneden, C., et al. 2001, AJ, 122, 1438
Johnson, C. I., McDonald, I., Pilachowski, C. A., et al. 2015, AJ, 149, 71
Knigge, C., Leigh, N., & Sills, A. 2009, Natur, 457, 288
Koch, A., & McWilliam, A. 2008, AJ, 135, 1551
Lane, R. R., Kiss, L. L., Lewis, G. F., et al. 2010, MNRAS, 401, 2521
Lanzoni, B., Sanna, N., Ferraro, F. R., et al. 2007, ApJ, 663, 1040
Lapenna, E., Mucciarelli, A., Lanzoni, B., et al. 2014, ApJ, 797, 124
Lombardi, J. C., Jr, Rasio, F. A., & Shapiro, S. L. 1995, ApJ, 445L, 117
Lombardi, J. C., Jr, Warren, J. S., Rasio, F. A., Sills, A., & Warren, A. R. 2002, ApJ, 568, 939
Lovisi, L., Mucciarelli, A., Ferraro, F. R., et al. 2010, ApJL, 719, L121
Mapelli, M., Ripamonti, E., Battaglia, G., et al. 2009, MNRAS, 396, 1771
Mapelli, M., Sigurdsson, S., Ferraro, F. R., et al. 2006, MNRAS, 373, 361
Mashonkina, L., Gehren, T., Shi, J.-R., Korn, A. J., & Grupp, F. 2011, A&A, 528, A87
Mathieu, R. D., & Geller, A. M. 2009, Natur, 462, 1032
McCarthy, J. K., & Nemec, J. M. 1997, ApJ, 482, 203
McCrea, W. H. 1964, MNRAS, 128, 147
Miocchi, P., Lanzoni, B., Ferraro, F. R., et al. 2013, ApJ, 774, 151
Miocchi, P., Pasquato, M., Lanzoni, B., et al. 2015, ApJ, 799, 44
Monelli, M., Cassisi, S., Mapelli, M., et al. 2012, ApJ, 744, 157
Mucciarelli, A. 2013, arXiv:1311.1403
Mucciarelli, A., Lapenna, E., Massari, D., Ferraro, F. R., & Lanzoni, B. 2015, ApJ, 801, 69
Mucciarelli, A., Lovisi, L., Ferraro, F. R., et al. 2014, ApJ, 797, 43
Mucciarelli, A., Pancino, E., Lovisi, L., Ferraro, F. R., & Lapenna, E. 2013, ApJ, 766, 78
Origlia, L., Ferraro, F. R., Fabbri, S., et al. 2014, A&A, 564, AA136
Origlia, L., Rood, R. T., Fabbri, S., et al. 2007, ApJL, 667, L85
Origlia, L., Rood, R. T., Fabbri, S., et al. 2010, ApJ, 718, 522
Pasquini, L., Avila, G., Allaert, E., et al. 2000, Proc. SPIE, 4008, 129
Pietrinferni, A., Cassisi, S., Salaris, M., & Castelli, F. 2006, ApJ, 642, 797
Preston, G. W., & Sneden, C. 2000, AJ, 120, 1014
Renzini, A., & Fusi Pecci, F. 1988, ARA&A, 26, 199
Robin, A. C., Reylé, C., Derrière, S., & Picaud, S. 2003, A&A, 409, 523
Sarajedini, A., et al. 2007, AJ, 133, 1658
Shara, M. M., Saffer, R. A., & Livio, M. 1997, ApL, 489, L59
Sills, A., Karakas, A., & Lattanzio, J. 2009, ApJ, 692, 1411
Stetson, P. B., & Pancino, E. 2008, PASP, 120, 1332
Thygesen, A. O., Sbordone, L., Andrievsky, S., et al. 2014, A&A, 572, AA108
Tian, B., Deng, L.-C., Han, Z.-W., & Zhang, X.-B. 2006, A&A, 455, 247
Xin, Y., Ferraro, F. R., Lu, P., et al. 2015, ApJ, 801, 67
Zinn, R., & King, C. R. 1982, ApJ, 262, 700